HHS Public Access

Author manuscript

Cell. Author manuscript; available in PMC 2015 August 28.

Published in final edited form as:

Cell. 2014 August 28; 158(5): 1148–1158. doi:10.1016/j.cell.2014.07.026.

A molecular framework for temperature-dependent gating of ion channels

Sandipan Chowdhury[*,±,†], **Brian W. Jarecki**[*,±,¥], and **Baron Chanda**[±,¶]

[†]Graduate Program in Biophysics, 1111 Highland Ave, School of Medicine and Public Health, University of Wisconsin, Madison, WI-53705

[±]Department of Neuroscience, 1111 Highland Ave, School of Medicine and Public Health, University of Wisconsin, Madison, WI-53705

Summary

Perception of heat or cold in higher organisms is mediated by specialized ion channels whose gating is exquisitely sensitive to temperature. The physicochemical underpinnings of this temperature-sensitive gating have proven difficult to parse. Here, we took a bottom-up protein design approach, and rationally engineered ion channels to activate in response to thermal stimuli. By varying amino acid polarities at sites undergoing state-dependent changes in solvation, we were able to systematically confer temperature-sensitivity to a canonical voltage-gated ion channel. Our results imply that the specific heat capacity change during channel gating is a major determinant of thermo-sensitive gating. We also show that reduction of gating charges amplifies temperature-sensitivity of designer channels which accounts for low voltage-sensitivity in all known temperature-gated ion channels. These emerging principles suggest a plausible molecular mechanism for temperature-dependent gating that reconcile how ion channels with an overall conserved transmembrane architecture may exhibit a wide range of temperature-sensing phenotypes.

Introduction

The ability to sense and respond to thermal stimuli is essential for an organism's survival. Not surprisingly, adaptive evolution has led to the emergence of specialized temperature-sensing mechanisms enabling organisms to rapidly detect noxious temperature stimuli. In higher organisms, this role is performed by members of a specialized family of ion channels - the TRP channels (Clapham, 2003; Patapoutian et al., 2003). Members of this family of

[¶]Address correspondence to chanda@wisc.edu.

[¥]Present address: Cellular Dynamics International, 525 Science Drive, Madison, WI 53711.

[*]Both these authors contributed equally to this effort.

Author Contributions: S.C. and B.C conceived and designed the project and the experiments; S.C. and B.W.J performed all the electrophysiology experiments and analyzed the data; S.C. made all the mutations for this project; S.C. performed the molecular simulations and polarity conservation analysis; S.C. and B.C. wrote the manuscript.

membrane proteins enable ions to flux across the membrane when stimulated by changes in temperature (Caterina et al., 1997; McKemy et al., 2002; Peier et al., 2002; Story et al., 2003). Recently, the calcium activated chloride channel, a member of the TMEM 16 family of ion channels, has been shown to be involved in heat sensitivity and possibly nociception (Cho et al., 2012). Several other ion channels, such as H_V (DeCoursey and Cherny, 1998), hERG (Vandenberg et al., 2006), K2P (Maingret et al., 2000) and ClC (Pusch et al., 1997) are known to be strongly modulated by changes in temperature. Moreover, several pathological mutations in the voltage-gated sodium channels (Na_V) have been identified, which enhance the temperature dependence of the Na_V channel activity (Dib-Hajj et al., 2008). Thus it raises an important question – is there a general mechanism which underlies temperature dependent gating of channels?

TRP channels have become model systems for studying temperature-gating in part due to their biological role in detecting thermal stimuli and unusually high temperature sensitivity. Approaches such as high throughput mutagenesis (Grandl et al., 2008; Grandl et al., 2010), chimeragenesis (Brauchi et al., 2006; Cordero-Morales et al., 2011; Yang et al., 2010; Yao et al., 2011) and deletion studies (Cui et al., 2012; Vlachova et al., 2003) have been combined with functional measurements to identify parts of the protein that are involved in temperature-dependent gating. These studies, however, cannot discriminate between effects on the temperature-sensor itself versus those on downstream elements involved in coupling putative thermo-sensors to the pore. In voltage-sensing or ligand-gated processes, it is possible to unequivocally determine the molecular nature of these sensors by observing gating charge movement or ligand binding directly. In contrast, the formidable technical challenge of calorimetrically measuring the heat associated with channel gating has seriously impaired the search of a physiological temperature-sensing domain. While it has been suggested that temperature-dependent gating in heat- and cold-sensing channels involves large scale rearrangements in a specialized domain (Brauchi et al., 2004; Yang et al., 2010; Yao et al., 2010, 2011), to date no consensus domain or motif has emerged as a candidate. Strikingly, TRPA1 in pit-bearing snakes are heat-sensitive channels (Gracheva et al., 2010) whereas the rat ortholog is a cold-sensitive channel (Story et al., 2003) implying that small changes in primary structure may underlie differences in temperature-sensitivity (Chen et al., 2013). Clapham and Miller (2011) have recently suggested that if specific heat capacity is taken into account, then it would be possible to generate a variety of temperature-sensitive phenotype without necessarily invoking a specialized modular thermal sensor (Cao et al., 2013; Liao et al., 2013; Long et al., 2007).

In structural biology, rational design serves as the benchmark for understanding the physical principles of protein folding and function. We hypothesize that a similar design approach may help illuminate the general molecular principles of temperature-dependent gating. Here, we redesigned a canonical voltage-gated ion channel, whose overall architecture is similar to TRP channel, into channels that are either gated by heat or cold. Our bottom-up design approach is based on the paradigm that solvation and desolvation of amino acids is associated with distinct changes in specific heat capacity (Privalov and Makhatadze, 1990). By systematically varying the polarity of residues that are likely to undergo changes in solvent accessibility during the gating process, we were able to control the temperature-sensitivity of channel gating. In addition, we illustrate how the principle of thermodynamic

coupling amplifies temperature-sensitivity when voltage-sensing gating charges are reduced. Together, our findings establish a molecular mechanism to understand how ion channels with similar overall form can sense heat and cold.

Results

The design principle

A central characteristic of temperature modulated ion channels is that upon changing the temperature, their relative open-probability *vs* voltage (P_OV) relationships shift along the voltage axis. For heat sensing channels, such as TRPV1, the P_OV curves shift left when the temperature is increased (Voets et al., 2004), reflecting that channel opening is energetically facilitated at elevated temperatures (Fig. 1a, top panel). Conversely, for cold sensing channels, such as TRPM8 (Fig. 1a, bottom panel), increase in temperature makes it harder for the channels to open and causes rightward shifts in their P_OV curves (Brauchi et al., 2004; Voets et al., 2004). Protein folding studies show that exposure of the hydrophobic core of the protein to the aqueous media results in organization of water molecules in the first solvation shells (Makhatadze and Privalov, 1993; Privalov and Makhatadze, 1993; Schellman et al., 1981). This process is also associated with changes in specific heat capacity (Baldwin, 1986; Privalov and Gill, 1988), which is what ultimately shapes the free-energy change *vs* temperature (ΔG *vs* T) profile of the folding/unfolding process. As shown in Fig. 1b, non-zero 'change in specific heat capacity' (ΔC_P) of any arbitrary process results in the ΔG *vs* T profile becoming curved (Clapham and Miller, 2011). The sign of ΔC_P determines whether the profile is convex-shaped or concave-shaped while its absolute value determines the degree of curvature (Fig. S1 a and b). Calorimetric studies show that solvation of hydrophobic residues is associated with a positive ΔC_P while that of polar/charged residues is associated with a negative ΔC_P (Makhatadze et al., 1990; Makhatadze and Privalov, 1990, 1994). This key observation formed the basis of our heuristic approach to design a temperature modulated ion channel.

The Shaker K_V channel has served as an exemplar ion channel, whose voltage-dependent gating has been extensively studied using electophysiological (Schoppa and Sigworth, 1998; Zagotta et al., 1994), spectroscopic (Pathak et al., 2007) and biochemical (Ahern and Horn, 2005; Xu et al., 2013) techniques. Of primary interest to us was the fact that its gating is only slightly modulated by change in temperature (Rodriguez and Bezanilla, 1996; Rodriguez et al., 1998). Upon lowering the temperature from 28°C to 8°C, the kinetics of activation and deactivation of its ionic currents is modestly decelerated (Fig. S1 c and b), its P_OV curve is right-shifted by less than 5mV and there is a slight reduction in its steepness (Fig. 1c). The relative insensitivity of the P_OV curve of the Shaker K_V channel complemented with the availability of wealth of structural (Butterwick and MacKinnon, 2010; Long et al., 2007) and functional (Alabi et al., 2007; Bosmans et al., 2008; Lu et al., 2002) data made it an excellent template to test our theories of physical basis of temperature dependent gating.

Voltage-dependent conformational changes of the Shaker K_V channel, underlying its transition between closed and open states, lead to changes in water accessibility in different parts of the protein (Jensen et al., 2010; Krepkiy et al., 2009; Larsson et al., 1996; Liu et al.,

1997; Starace et al., 1997). We reasoned that substitution of key residues, in regions which undergo increased solvation when channels open, with hydrophobic residues will confer a positive ΔC_P to the overall gating process while polar residues at similar locations will confer a negative ΔC_P. Although the individual contributions of polar residues to negative ΔCp may not be large, a decrease in the positive component will also make the net ΔCp associated with channel opening negative (see analysis in Supplementary Material). Such substitutions should thus sensitize voltage dependent gating to changes in temperature but the temperature sensing phenotype (i.e. cold or heat sensing) will depend on the polarity of perturbation. Conversely, perturbations at sites which undergo desolvation during channel opening, should also sensitize to temperature, although, hydrophobic and polar substitutions will now have an opposite impact on ΔC_P.

We chose to target sites within the voltage-sensing domain (VSD) of the Shaker K_V channel and perturb them to design a temperature-sensitive K_V channel. Our choice of the VSD over the pore domain was prompted by two factors. First, accessibility studies of thiol-modifying reagents and protons to substituted cysteines and histidines, respectively, in the VSDs, complemented with computational models of hydrated VSDs, suggest the presence of water accessible crevices within the VSD (Fig. 1d) which undergo structural reorganization when the channel opens (Li et al., 2014b; Nguyen and Horn, 2002; Schonherr et al., 2002; Starace and Bezanilla, 2004). Such processes would likely be associated with changes in accessibility of residues in the VSD. Second, the VSD, in general appears to be more resilient to perturbations than the pore domain as suggested by earlier studies which have reported that polar perturbations in the pore domain frequently compromises functional expression of channels (Hackos et al., 2002).

The specific sites within the VSD to be perturbed in this study were chosen based on two considerations. We reasoned that polar sites buried within the proteinaceous core of the VSD are likely to be the primary determinants of water occupancy in the voltage-sensing crevices. To identify such sites, using the structure of the VSD of the $K_V1.2/2.1$ paddle chimera, we computed the fractional buried surface area of each residue (Fig. 1e). Residues for which the buried fractions were > 0.8 were classified as buried residues. Next, using a previously reported alignment of 360 K_V channel sequences (Lee et al., 2009), we computed the polarity conservation index (PCI) of each of the sites in the VSD (see Extended experimental procedures in Supplementary Material). PCI of each site reflects the enrichment of polar/hydrophobic residues at a given site, based on evolutionary information. For each site, PCI > 1 reflects a strong enrichment of highly polar/charged residues, PCI between 0.3 and 1 reflects an enrichment of polar residues, while PCI < -0.3 suggests an enrichment of highly hydrophobic residues. Eight sites located in the S1-S3 segments of the VSD for which the fractional buried surface area > 0.8 and PCI > 0.3 were selected for experimental analysis (Fig. 1d and e).

Influence of residues in S1-S3

The three sites, S240, E293 and Y323, in the S1, S2 and S3 segments respectively were individually mutated to residues of varying polarity, beginning with a hydrophobic residue (Fig. 2a-c, top panel) and leading on to more polar residues (Fig. 2a-c, lower panels). The

relative-open probability vs voltage ($P_O V$) relationships of each of the mutants were measured at two different temperatures, 8°C and 28°C (Fig. 2a-c, blue and red curves respectively, Fig. S2). Several of these mutations resulted in significant shifts in the $P_O V$ curves (Table S1). For instance, upon heating (from 8°C to 28°C), the E293I mutant results in a ∼20mV rightward shift in the $P_O V$ curve (Fig. 2b, top panel) while the Y323I mutant causes a ∼30mV leftward shift. The change in the median voltage of channel opening upon heating ($\Delta V_M = V_M(28°C) - V_M(8°C)$) due to the different perturbations at each of the three sites are summarized in Fig. 2d, where ΔV_M due to each perturbation is plotted against the hydrophobicity of the perturbing residue in accordance with the biological hydrophobicity scale proposed by von Heijne and colleagues (Hessa et al., 2005). We hereafter refer to this as the H-vH scale.

A strong positive correlation was observed with the Y323 mutants (Fig. 2d, right panel) which indicates that increasing the polarity of the site causes the channel to switch from being heat to cold sensitive. Furthermore, we also observe that the V_M, at 28°C, for the different mutations at this site is also correlated with polarity (Fig. 2e). Together, these data suggest that the 323 site undergoes at least partial desolvation upon channel activation. A hydrophobic residue at such a site would thus confer a negative ΔC_P to channel gating while a polar residue would impart a positive ΔC_P. As shown in ΔG vs T plot (Fig. 1c) channel gating with positive ΔC_P will render the channel cold sensitive (within 8°C to 28°C) while a negative ΔC_P will make activation heat-sensitive. In contrast to the extracellular 323 site, we observe that ΔV_M is negatively correlated with changes in polarity at the intracellular 293 position (Fig. 2d center panel) and so is V_M at 28°C except for Gln substitution. This scenario can be explained if channel activation causes increased solvation of the site such that Ile substitution is associated with positive ΔC_p and His/Gln substitution has a negative ΔC_p.

For the S240 site (Fig. 2d, left panel), although V_M is correlated with polarity, ΔV_M is not. This could arise in instances wherein the site undergoes a change in polarity of the environment but its solvation status does not change. Other sites in the VSD, S233 (in S1), E283 (in S2), N313, D316 and T326 (all in S3), when mutated either did not yield functional channels (Table S1) or their $P_O V$ curves were virtually temperature independent (Fig. S2g). Interestingly, hydrophobic mutations at sites (S240, Y323 and T326) in the external crevice of the VSD, render channel opening (at 28°C) more favorable relative to polar mutations (Fig. S2h). Conversely, for the sites in the internal crevice (S233, E293 and N313), hydrophobic mutations make channel opening (at 28°C) less favorable, relative to polar mutations (Fig. S2i). This position dependence of perturbations suggests that there are complementary changes in solvation of internal and external water-filled crevices of the VSD during channel activation. These findings are consistent with the prevailing notion that the outward S4 movement relative to the S1-S3 segments upon depolarization increases the volume of the internal water accessible compartment while concomitantly decreasing that of the outside facing crevice (Li et al., 2014a; Li et al., 2014b).

Influence of hydrophobic residues in S4

Structure-function studies reveal that the hydrophobic residues between the principal gating charges on the S4 segment become exposed to a more polar environment when the channel activates (Xu et al., 2010; Xu et al., 2013). Such state-dependent changes in polarity at these sites make them suitable candidates to test for temperature-dependence. We created three hextuplet mutants, where the six uncharged residues between the gating charges were all mutated to Ile, Met or Ala. Measurements of the P_OV curves for each of these mutants (Fig. 3a) showed that decreasing the polarity of the perturbation left shifts the P_OV curves of the channel (at 28°C) and concomitantly renders the channel more heat sensitive (Fig. S3a). Next, we generated three quadruplet mutants, where four uncharged residues between the first and third gating charge (R362 and R368 respectively) were all mutated to Ile, Met or Ala. The P_OV curves of these three mutants (Fig. 3b) follow the overall trend of the heat sensitivities of the hextuplets, with the Ala mutant exhibiting the most left shifted PoV curve (at 28°C) and the largest heat sensitivity (∼28mV) (Fig. S3b). These observations imply that upon channel activation there is an increase in average solvation of these sites. However, unlike the 323 and 293 sites, there is no switch in temperature-sensitivity across the spectrum of perturbations. These observations can be reconciled with our original hypothesis if we consider that the perturbations are not only introducing new ΔC_p components but in some cases they can also subtract pre-existing ΔCp components associated with channel gating (see Supplementary Analysis section in Extended experimental procedures and Fig. S1)

To test the position dependence of the hydrophobic residues in S4, we mutated each intervening pair to create three sets of doublets (X2Top, X2Mid and X2Bot). Perturbations were made to four different amino acids, namely, Ile, Met, Ala, Ser, and in each of the twelve cases we measured the ΔV_M due a change in temperature from 8°C to 28°C (Fig. S3c-k). For the middle doublets, although the temperature dependent shifts of the P_OV curves are not polarity correlated, the V_M values (at 28°C) for different perturbations decrease as the polarity of these middle doublets increase (Fig. 3c, d, center panels). This selective effect of the perturbations on V_M suggests that the middle doublets behave as the S240 site (Fig. 2d and e, left panels). For the Top and Bottom doublets, ΔV_M exhibits a negative correlation with the polarity of perturbation although the V_M does not appear correlated (Fig. 3c, left and right panels). V_M is governed by both changes in solvation status as well as interactions with other parts of the protein and lipids. Although polarity correlated temperature-dependence of activation suggests that these sites are undergoing changes in solvation, other protein-protein or protein-lipid interactions are primary determinants of the set-point for channel opening(Smith-Maxwell et al., 1998; Xu et al., 2013). These experiments also highlight that relatively few perturbations can result in large temperature dependent shifts in the P_OV curves (Fig. 3e and Fig. S3), as seen with the S2Bot mutant (Fig. 3e, right panel) for which a 20°C change in temperature results in ∼75mV shift in the P_OV curves.

Enhancement of temperature sensitivity

Since temperature-dependent change in ΔG of channel gating is directly proportional to ΔC_P, we ask whether the temperature-sensitivity of our temperature-sensitive mutants can be

further raised by combining them since ΔC_P values should be additive. A combination of two heat sensitive mutants, Y323I and S2Mid results in a channel whose P_OV curve is dramatically left shifted (~56 mV) upon heating (Fig. 4a). We observed a similar large temperature-dependent shift when we generate a second combination mutant by combining the perturbations Y323I and M6 (the S4 hextuplet Met mutant, Fig. 2b). The temperature dependent shift for the resultant mutant was so large that we were unable to reliably measure the full P_OV curve at 8°C. Current measurements at 28°C and 15°C (Fig. 4b) shows that increasing the temperature shifts the P_OV leftward by ~35 mV. Thus, both combination mutants show much larger temperature-sensitivity than the individual mutants which is expected if ΔC_P influences the slope of the ΔG vs. T plots.

A hallmark of temperature dependent channels is that change in temperature drastically alters the magnitude of ion flux through the channel. To gauge the extent of temperature sensitization of our engineered channels, we performed temperature ramp experiments. For the wild-type channel, a 20°C decrease in temperature causes ~2.2 fold reduction in outward currents (at -20mV) in all likelihood due to the change in single channel conductance. In comparison, S2Bot (i.e. V369S/F370S) and Y323I/M6, the same change in temperature led to a ~30 and ~36 fold reduction in the current, respectively (Fig. 4c and d). A semi-logarithmic plot of the fraction of current at each temperature (relative to current at 28°C) *vs* inverse of temperature, for each of the two mutants (Fig. 4c and d) shows steep temperature dependence in both cases. In the temperature range of 10-14°C, Q_{10} value of the outward currents elicited by the 100ms depolarizing pulses at -20mV is 18.3 and 15.5 for the S2Bot and Y323I/M6 mutants respectively. These Q_{10} values are much larger than that of the WT Shaker and are comparable to those reported for thermoTRPs (Clapham and Miller, 2011). These findings engenders the view that modest structural changes in critical parts of a channel undergoing state dependent changes in solvation may underlie the temperature responsiveness of the channel (Clapham and Miller, 2011).

Role of gating charges in temperature modulation

Temperature-dependent shift in the midpoint of activation curves, ΔV_M, is governed by the ratio $f(\Delta S, \Delta C_P)/z$, where '$f(\Delta S, \Delta C_P)$' is a function of the change in entropy and/or heat capacity change of channel gating and 'z' is its apparent voltage-sensitivity(Latorre et al., 2007; Rodriguez and Bezanilla, 1996; Rodriguez et al., 1998; Voets et al., 2004). Thus, if the voltage-sensing charges are neutralized, there will a reduction in 'z' and the sensitivity of the channel to changes in temperature will be enhanced. To test this principle, we mutated the four S4 charges (R362, R365, R368 and R371), to either Ala and Gln (or Asn for R368). The P_OV curves of each of these mutants were virtually non-responsive to changes in temperature (Fig. S4 and Fig. 5a and b) except for R365A, which shows mild cold sensitivity (~ 10mV shift). Next, we introduced the R368N and R371Q mutations in the background of the heat sensitive Y323I mutation and recorded their P_OV curves. Strikingly both mutants were significantly more heat sensitive than the Y323I mutant alone (Fig. 5c and d). To further investigate this charge-dependent enhancement of temperature sensitivity, we combined the R371Q mutant with the modestly heat sensitive S2Mid mutant and the modestly cold sensitive Y323Q mutant and assessed the temperature dependent shifts in their P_OV curves. As in previous instances, the modestly heat sensitive mutant was rendered

significantly more heat sensitive by the R371Q neutralization (Fig. 5e) while the modestly cold sensitive mutant became significantly more cold sensitive in the background of the R371Q mutant (Fig. 5f).

The magnitude of temperature dependent shifts in the $P_O V$ curves due to the mutations (namely, Y323I, Y323Q and S2Mid) when introduced in the background of a charge neutralizations were plotted against the shifts observed in the wild type background (Fig. 5g). The plot shows a linear relationship with a regression slope of ~2 which implies that in every case single charge neutralization (R368N or R371Q) approximately doubles the temperature dependent shifts in the $P_O V$ curves. Such a charge dependent effect is in complete agreement with the thermodynamic predictions, described in the simulated V_M *vs* temperature profiles shown in Fig. 5h. For two processes with identical ΔG *vs* T profiles, the V_M *vs* T profiles will be more curved (and/or steep) for the process which has a lower voltage-sensitivity. As a result, the mutant with a lower voltage-sensitivity will be much more sensitive to changes in temperature than those with a higher voltage-sensitivity. To the best of our knowledge, these results are the first experimental demonstration of the inverse relationship between temperature-sensitivity and voltage-sensing.

Discussion

Thermodynamic descriptions of temperature dependent activation of ion channels based on van't Hoff analysis shows that the gating of these channels are associated with large changes in enthalpy. These large enthalpy values must be compensated by large changes in entropy to keep the process of channel gating reversible at physiological temperatures. However, molecular origins of such large changes in enthalpy and entropy remain an enigma. Clapham and Miller recently pointed out (Clapham and Miller, 2011) the importance of specific heat capacity change accompanying channel gating as a primary determinant for the large changes in the enthalpy and entropy of channel gating and thus the overall temperature dependence of ion channel activity. However, measuring ΔC_P of channel gating of the natively temperature sensitive channels (e.g. thermoTRPs) has been an enormous challenge because of two fundamental reasons. First, an accurate estimate of ΔG of gating, at different temperatures, necessarily requires experimental measurements of either the conjugate displacements associated with a stimulus or heat exchange during gating, both of which are non-trivial. Second, accurate ΔG estimates need to be obtained at temperatures close to T_C (the temperature at which the ΔG *vs* T profile is at maximum or minimum) because, further away from T_C, ΔG *vs* T profiles become quasi-linear and ΔC_P cannot be accurately calculated. To date, non-monotonicity of ΔG vs T curves have not been observed which would suggest that the T_C is likely to be outside the experimentally accessible temperature range.

To test the role of ΔC_P on temperature-dependent gating of ion channel, we have developed a model system that allows us to modulate the ΔC_P associated with the gating process in a somewhat well-defined manner and test its effects on channel gating. Our approach exploits the prior knowledge that ΔC_P of solvation of polar and non-polar residues are opposite in sign and during voltage-dependent activation certain regions of the Shaker potassium channel undergo changes in water accessibility (Fig. 6). We identify multiple positions on

voltage-sensing domain at which perturbations introduce large temperature dependent shifts on the channel activation curves, in a polarity correlated fashion. It is clear, however, that in some instances, temperature dependent effects on gating do not parallel polarity and this might be due to multiple reasons. First, P_OV (or conductance-voltage) curves do not reflect the full energetics of channel activation of multi-state systems (Chowdhury and Chanda, 2012, 2013) and may not accurately recapitulate temperature dependent changes in free-energy. Second, the substituted side-chains may become partially solvent accessible which would reduce their contribution to ΔC_P of solvation. Third, the properties of the water molecules in the crevices may be different from that of the bulk water (Franzese and Rubi, 2008) which could result in anomalous heat capacity changes. Finally, we also have to take into account the pKa of titratable side-chains which are significantly dependent on their local environments. Despite these caveats, our results show that relatively few mutations (1 to 7 per subunit) can profoundly alter the temperature sensing phenotype of the channel (as exhibited by the Y323I, S2Bot, Y323I-S2mid, Y323I-M6 mutants) implying that large conformational changes in the protein is not a pre-requisite for strong temperature dependent gating.

Our experiments also shed light on the major influence of voltage-sensing charges on temperature dependence of P_OV curves. Although an inverse relationship between voltage and temperature sensitivity of a channel has been proposed earlier in the context of TRP channels (Latorre et al., 2007; Voets et al., 2004), direct experimental evidence in support of such a hypothesis has been lacking, in part due to the uncertainty regarding the identity of gating charges in the thermoTRPs. However, the charge carrying residues in the Shaker K_V channel are well known which enables us to directly test this hypothesis. Gating-charge neutralizations in the wild-type channels do not exhibit temperature-sensitive responses whereas when introduced in the background of heat- or cold-sensitized mutants, the resultant mutants exhibit substantially enhanced temperature sensitivity highlighting the crucial but indirect role of charges on temperature gating.

In conclusion, through the characterization of the relative open-probability *vs* voltage relationships of several targeted mutants of the Shaker K_V channel, at two different temperatures, we have elucidated a fundamental physical principle underlying temperature modulation of voltage-dependent gating. The idea that relatively modest conformational changes which lead to change in solvation of residues can massively enhance the temperature sensitivity of the channel is important as it illustrates the structural generality of temperature-dependent gating. This is a crucial point as traditional voltage and ligand gated ion channels harbor specialized structural domains which serve as sensors. Temperature dependent gating of naturally heat or cold sensing ion channels could thus arise out of small conformational changes occurring in different parts, leading to large overall heat capacity changes. Consistent with such a proposition, perturbations at different locations of the TRPV1 channel have been shown to alter its temperature dependent gating. Our findings illustrate an alternate mechanism wherein temperature sensitivity is conferred by multiple temperature-sensing microdomains distributed over the whole channel, rather than a distinct temperature-sensing domain.

Experimental Procedures

Identification of polar buried residues in the VSD

The residue-specific solvent accessible surface area of the VSD of K_V 1.2/2.1 paddle-chimera structure (PDB-ID: 2R9R, residues 159-310) was computed using VMD (Humphrey et al., 1996) and normalized using standard surface area of each amino acid residue (probe radius 1.4 Å). For the polarity conservation index (PCI) calculation, a multiple sequence alignment of 360 K_V channel homologs (Lee et al., 2009) was used to compute the gap-corrected position specific frequency of each amino acid (a) and each position of the alignment (i), $f_i^{(a)}$ (gap-correction normalizes the raw frequency scores at each position of the alignment with $1 - f_i^{(gap)}$). This was subsequently used to compute the polarity conservation index (PCI) of each site as: $\sum_{(a)} h_{(a)} f_i^{(a)}$, where the summation is over all 20 amino acids and $h_{(a)}$ indicates the hydrophobicity score of the amino acid (a) (according to the the Hessa von-Heijne (H-vH) scale (Hessa et al., 2005)).

Molecular Biology and Electrophysiology

All mutations were introduced in the background of the Shaker inactivation removed construct in the pBSTA vector using PCR-based mutagenesis and confirmed with sequencing of the cDNA. Linearized cDNA was in vitro transcribed with T7 polymerase using the mMessage mMachine transcription kit (Ambion). In vitro transcribed mRNA was injected in de-vitellinated Xenopus laevis oocytes (1–10ng) and currents were measured 12-48 hrs post-injection on a cut-open oocyte voltage clamp (COVC) set up (CA-1B; Dagan Corporation). The recording temperature was controlled and altered using a peltier device, fitted onto the COVC recording chamber. For all electrophysiological recordings, the internal solution used was 105 mM KMeS, 20 mM HEPES, 2 mM EGTA (pH: 7.2) and the external solution was either 105 mM KMeS, 20 mM HEPES, 2 mM $Ca(OH)_2$ (pH 7.2) or 10 mM KMeS/95 mM NMG-MeS, 20 mM HEPES, 2 mM $Ca(OH)_2$ (pH 7.2). In all experiments, the holding voltage was -120 mV and currents were elicited by depolarization pulses, 50-500ms long, in 5 mV increments (unless otherwise mentioned). P/-4 leak subtraction protocol was used to remove linear leak/capacitive currents. Analogue signals were sampled at 20-250 kHz with a Digidata 1440 interface (Molecular Devices) and low-pass filtered at 10 kHz. Peak tail currents (at -120mV) were used to generate the relative open-probability *vs* voltage curves, from which the median voltage of channel opening, V_M, was extracted by measuring the area between the curve and the ordinate axis as described earlier (Chowdhury and Chanda, 2012, 2013). For the temperature ramp experiments, the temperature was initially held at 28°C and ramped to 8°C at a speed of ∼1°C/15 sec; the holding voltage was -120mV, and 100ms depolarization pulses to -20mV (close to the V_M of the wild-type Shaker K_V channel) was applied every 1°C.

Supplementary Material

Refer to Web version on PubMed Central for supplementary material.

Acknowledgments

We thank Drs. Q. Cui, M. Jackson, T. Record, C. Czajkawoski and members of the Chanda laboratory for their comments and discussions; R.R. Trivedi (Khorana fellow) for early help with data collection; K.M. Schuldt and T.R. Lingle for technical assistance. The project was supported by funds from the National Institutes of Health (RO1-NS081293), Shaw Scientist award and Vilas Research foundation to B.C. B.W.J was partially supported by NIH training grant (5T32HL007936-09).

References

Ahern CA, Horn R. Focused electric field across the voltage sensor of potassium channels. Neuron. 2005; 48:25–29. [PubMed: 16202706]

Alabi AA, Bahamonde MI, Jung HJ, Kim JI, Swartz KJ. Portability of paddle motif function and pharmacology in voltage sensors. Nature. 2007; 450:370–375. [PubMed: 18004375]

Baldwin RL. Temperature dependence of the hydrophobic interaction in protein folding. Proc Natl Acad Sci U S A. 1986; 83:8069–8072. [PubMed: 3464944]

Bosmans F, Martin-Eauclaire MF, Swartz KJ. Deconstructing voltage sensor function and pharmacology in sodium channels. Nature. 2008; 456:202–208. [PubMed: 19005548]

Brauchi S, Orio P, Latorre R. Clues to understanding cold sensation: thermodynamics and electrophysiological analysis of the cold receptor TRPM8. Proc Natl Acad Sci U S A. 2004; 101:15494–15499. [PubMed: 15492228]

Brauchi S, Orta G, Salazar M, Rosenmann E, Latorre R. A hot-sensing cold receptor: C-terminal domain determines thermosensation in transient receptor potential channels. J Neurosci. 2006; 26:4835–4840. [PubMed: 16672657]

Butterwick JA, MacKinnon R. Solution structure and phospholipid interactions of the isolated voltage-sensor domain from KvAP. J Mol Biol. 2010; 403:591–606. [PubMed: 20851706]

Cao E, Liao M, Cheng Y, Julius D. TRPV1 structures in distinct conformations reveal activation mechanisms. Nature. 2013; 504:113–118. [PubMed: 24305161]

Caterina MJ, Schumacher MA, Tominaga M, Rosen TA, Levine JD, Julius D. The capsaicin receptor: a heat-activated ion channel in the pain pathway. Nature. 1997; 389:816–824. [PubMed: 9349813]

Chen J, Kang D, Xu J, Lake M, Hogan JO, Sun C, Walter K, Yao B, Kim D. Species differences and molecular determinant of TRPA1 cold sensitivity. Nat Commun. 2013; 4:2501. [PubMed: 24071625]

Cho H, Yang YD, Lee J, Lee B, Kim T, Jang Y, Back SK, Na HS, Harfe BD, Wang F, et al. The calcium-activated chloride channel anoctamin 1 acts as a heat sensor in nociceptive neurons. Nat Neurosci. 2012; 15:1015–1021. [PubMed: 22634729]

Chowdhury S, Chanda B. Estimating the voltage-dependent free energy change of ion channels using the median voltage for activation. J Gen Physiol. 2012; 139:3–17. [PubMed: 22155736]

Chowdhury S, Chanda B. Free-energy relationships in ion channels activated by voltage and ligand. J Gen Physiol. 2013; 141:11–28. [PubMed: 23250866]

Clapham DE. TRP channels as cellular sensors. Nature. 2003; 426:517–524. [PubMed: 14654832]

Clapham DE, Miller C. A thermodynamic framework for understanding temperature sensing by transient receptor potential (TRP) channels. Proc Natl Acad Sci U S A. 2011; 108:19492–19497. [PubMed: 22109551]

Cordero-Morales JF, Gracheva EO, Julius D. Cytoplasmic ankyrin repeats of transient receptor potential A1 (TRPA1) dictate sensitivity to thermal and chemical stimuli. Proc Natl Acad Sci U S A. 2011; 108:E1184–1191. [PubMed: 21930928]

Cui Y, Yang F, Cao X, Yarov-Yarovoy V, Wang K, Zheng J. Selective disruption of high sensitivity heat activation but not capsaicin activation of TRPV1 channels by pore turret mutations. J Gen Physiol. 2012; 139:273–283. [PubMed: 22412190]

DeCoursey TE, Cherny VV. Temperature dependence of voltage-gated H+ currents in human neutrophils, rat alveolar epithelial cells, and mammalian phagocytes. J Gen Physiol. 1998; 112:503–522. [PubMed: 9758867]

Dib-Hajj SD, Yang Y, Waxman SG. Genetics and molecular pathophysiology of Na(v)1.7-related pain syndromes. Adv Genet. 2008; 63:85–110. [PubMed: 19185186]

Franzese, G.; Rubi, M., editors. Aspects of Physical Biology: Biological Water, Protein Solutions, Transport and Replication. Springer; Berlin Heidelberg: 2008.

Gracheva EO, Ingolia NT, Kelly YM, Cordero-Morales JF, Hollopeter G, Chesler AT, Sanchez EE, Perez JC, Weissman JS, Julius D. Molecular basis of infrared detection by snakes. Nature. 2010; 464:1006–1011. [PubMed: 20228791]

Grandl J, Hu H, Bandell M, Bursulaya B, Schmidt M, Petrus M, Patapoutian A. Pore region of TRPV3 ion channel is specifically required for heat activation. Nat Neurosci. 2008; 11:1007–1013. [PubMed: 19160498]

Grandl J, Kim SE, Uzzell V, Bursulaya B, Petrus M, Bandell M, Patapoutian A. Temperature-induced opening of TRPV1 ion channel is stabilized by the pore domain. Nat Neurosci. 2010; 13:708–714. [PubMed: 20414199]

Hackos DH, Chang TH, Swartz KJ. Scanning the intracellular S6 activation gate in the shaker K+ channel. J Gen Physiol. 2002; 119:521–532. [PubMed: 12034760]

Hessa T, Kim H, Bihlmaier K, Lundin C, Boekel J, Andersson H, Nilsson I, White SH, von Heijne G. Recognition of transmembrane helices by the endoplasmic reticulum translocon. Nature. 2005; 433:377–381. [PubMed: 15674282]

Humphrey W, Dalke A, Schulten K. VMD: visual molecular dynamics. J Mol Graph. 1996; 14:33–38. 27–38. [PubMed: 8744570]

Jensen MO, Borhani DW, Lindorff-Larsen K, Maragakis P, Jogini V, Eastwood MP, Dror RO, Shaw DE. Principles of conduction and hydrophobic gating in K+ channels. Proc Natl Acad Sci U S A. 2010; 107:5833–5838. [PubMed: 20231479]

Krepkiy D, Mihailescu M, Freites JA, Schow EV, Worcester DL, Gawrisch K, Tobias DJ, White SH, Swartz KJ. Structure and hydration of membranes embedded with voltage-sensing domains. Nature. 2009; 462:473–479. [PubMed: 19940918]

Larsson HP, Baker OS, Dhillon DS, Isacoff EY. Transmembrane movement of the shaker K+ channel S4. Neuron. 1996; 16:387–397. [PubMed: 8789953]

Latorre R, Brauchi S, Orta G, Zaelzer C, Vargas G. ThermoTRP channels as modular proteins with allosteric gating. Cell Calcium. 2007; 42:427–438. [PubMed: 17499848]

Lee SY, Banerjee A, MacKinnon R. Two separate interfaces between the voltage sensor and pore are required for the function of voltage-dependent K(+) channels. PLoS Biol. 2009; 7:e47. [PubMed: 19260762]

Li Q, Wanderling S, Paduch M, Medovoy D, Singharoy A, McGreevy R, Villalba-Galea CA, Hulse RE, Roux B, Schulten K, et al. Structural mechanism of voltage-dependent gating in an isolated voltage-sensing domain. Nat Struct Mol Biol. 2014a; 21:244–252. [PubMed: 24487958]

Li Q, Wanderling S, Sompornpisut P, Perozo E. Structural basis of lipid-driven conformational transitions in the KvAP voltage-sensing domain. Nat Struct Mol Biol. 2014b; 21:160–166. [PubMed: 24413055]

Liao M, Cao E, Julius D, Cheng Y. Structure of the TRPV1 ion channel determined by electron cryo-microscopy. Nature. 2013; 504:107–112. [PubMed: 24305160]

Liu Y, Holmgren M, Jurman ME, Yellen G. Gated access to the pore of a voltage-dependent K+ channel. Neuron. 1997; 19:175–184. [PubMed: 9247273]

Long SB, Tao X, Campbell EB, MacKinnon R. Atomic structure of a voltage-dependent K+ channel in a lipid membrane-like environment. Nature. 2007; 450:376–382. [PubMed: 18004376]

Lu Z, Klem AM, Ramu Y. Coupling between voltage sensors and activation gate in voltage-gated K+ channels. J Gen Physiol. 2002; 120:663–676. [PubMed: 12407078]

Maingret F, Lauritzen I, Patel AJ, Heurteaux C, Reyes R, Lesage F, Lazdunski M, Honore E. TREK-1 is a heat-activated background K(+) channel. EMBO J. 2000; 19:2483–2491. [PubMed: 10835347]

Makhatadze GI, Gill SJ, Privalov PL. Partial molar heat capacities of the side chains of some amino acid residues in aqueous solution. The influence of the neighboring charges. Biophys Chem. 1990; 38:33–37. [PubMed: 17056435]

Makhatadze GI, Privalov PL. Heat capacity of proteins. I. Partial molar heat capacity of individual amino acid residues in aqueous solution: hydration effect. J Mol Biol. 1990; 213:375–384. [PubMed: 2342113]

Makhatadze GI, Privalov PL. Contribution of hydration to protein folding thermodynamics. I. The enthalpy of hydration. J Mol Biol. 1993; 232:639–659. [PubMed: 8393940]

Makhatadze GI, Privalov PL. Hydration effects in protein unfolding. Biophys Chem. 1994; 51:291–304. discussion 304-299. [PubMed: 7919040]

McKemy DD, Neuhausser WM, Julius D. Identification of a cold receptor reveals a general role for TRP channels in thermosensation. Nature. 2002; 416:52–58. [PubMed: 11882888]

Nguyen TP, Horn R. Movement and crevices around a sodium channel S3 segment. J Gen Physiol. 2002; 120:419–436. [PubMed: 12198095]

Patapoutian A, Peier AM, Story GM, Viswanath V. ThermoTRP channels and beyond: mechanisms of temperature sensation. Nat Rev Neurosci. 2003; 4:529–539. [PubMed: 12838328]

Pathak MM, Yarov-Yarovoy V, Agarwal G, Roux B, Barth P, Kohout S, Tombola F, Isacoff EY. Closing in on the resting state of the Shaker K(+) channel. Neuron. 2007; 56:124–140. [PubMed: 17920020]

Peier AM, Moqrich A, Hergarden AC, Reeve AJ, Andersson DA, Story GM, Earley TJ, Dragoni I, McIntyre P, Bevan S, et al. A TRP channel that senses cold stimuli and menthol. Cell. 2002; 108:705–715. [PubMed: 11893340]

Privalov PL, Gill SJ. Stability of protein structure and hydrophobic interaction. Adv Protein Chem. 1988; 39:191–234. [PubMed: 3072868]

Privalov PL, Makhatadze GI. Heat capacity of proteins. II. Partial molar heat capacity of the unfolded polypeptide chain of proteins: protein unfolding effects. J Mol Biol. 1990; 213:385–391. [PubMed: 2160545]

Privalov PL, Makhatadze GI. Contribution of hydration to protein folding thermodynamics. II. The entropy and Gibbs energy of hydration. J Mol Biol. 1993; 232:660–679. [PubMed: 8393941]

Pusch M, Ludewig U, Jentsch TJ. Temperature dependence of fast and slow gating relaxations of ClC-0 chloride channels. J Gen Physiol. 1997; 109:105–116. [PubMed: 8997669]

Rodriguez BM, Bezanilla F. Transitions near the open state in Shaker K(+)-channel: probing with temperature. Neuropharmacology. 1996; 35:775–785. [PubMed: 8938710]

Rodriguez BM, Sigg D, Bezanilla F. Voltage gating of Shaker K+ channels. The effect of temperature on ionic and gating currents. J Gen Physiol. 1998; 112:223–242. [PubMed: 9689029]

Schellman JA, Lindorfer M, Hawkes R, Grutter M. Mutations and protein stability. Biopolymers. 1981; 20:1989–1999. [PubMed: 7306671]

Schonherr R, Mannuzzu LM, Isacoff EY, Heinemann SH. Conformational switch between slow and fast gating modes: allosteric regulation of voltage sensor mobility in the EAG K+ channel. Neuron. 2002; 35:935–949. [PubMed: 12372287]

Schoppa NE, Sigworth FJ. Activation of Shaker potassium channels. III. An activation gating model for wild-type and V2 mutant channels. J Gen Physiol. 1998; 111:313–342. [PubMed: 9450946]

Smith-Maxwell CJ, Ledwell JL, Aldrich RW. Uncharged S4 residues and cooperativity in voltage-dependent potassium channel activation. J Gen Physiol. 1998; 111:421–439. [PubMed: 9482709]

Starace DM, Bezanilla F. A proton pore in a potassium channel voltage sensor reveals a focused electric field. Nature. 2004; 427:548–553. [PubMed: 14765197]

Starace DM, Stefani E, Bezanilla F. Voltage-dependent proton transport by the voltage sensor of the Shaker K+ channel. Neuron. 1997; 19:1319–1327. [PubMed: 9427254]

Story GM, Peier AM, Reeve AJ, Eid SR, Mosbacher J, Hricik TR, Earley TJ, Hergarden AC, Andersson DA, Hwang SW, et al. ANKTM1, a TRP-like channel expressed in nociceptive neurons, is activated by cold temperatures. Cell. 2003; 112:819–829. [PubMed: 12654248]

Vandenberg JI, Varghese A, Lu Y, Bursill JA, Mahaut-Smith MP, Huang CL. Temperature dependence of human ether-a-go-go-related gene K+ currents. Am J Physiol Cell Physiol. 2006; 291:C165–175. [PubMed: 16452156]

Vlachova V, Teisinger J, Susankova K, Lyfenko A, Ettrich R, Vyklicky L. Functional role of C-terminal cytoplasmic tail of rat vanilloid receptor 1. J Neurosci. 2003; 23:1340–1350. [PubMed: 12598622]

Voets T, Droogmans G, Wissenbach U, Janssens A, Flockerzi V, Nilius B. The principle of temperature-dependent gating in cold- and heat-sensitive TRP channels. Nature. 2004; 430:748–754. [PubMed: 15306801]

Xu Y, Ramu Y, Lu Z. A shaker K+ channel with a miniature engineered voltage sensor. Cell. 2010; 142:580–589. [PubMed: 20691466]

Xu Y, Ramu Y, Shin HG, Yamakaze J, Lu Z. Energetic role of the paddle motif in voltage gating of Shaker K(+) channels. Nat Struct Mol Biol. 2013; 20:574–581. [PubMed: 23542156]

Yang F, Cui Y, Wang K, Zheng J. Thermosensitive TRP channel pore turret is part of the temperature activation pathway. Proc Natl Acad Sci U S A. 2010; 107:7083–7088. [PubMed: 20351268]

Yao J, Liu B, Qin F. Kinetic and energetic analysis of thermally activated TRPV1 channels. Biophys J. 2010; 99:1743–1753. [PubMed: 20858418]

Yao J, Liu B, Qin F. Modular thermal sensors in temperature-gated transient receptor potential (TRP) channels. Proc Natl Acad Sci U S A. 2011; 108:11109–11114. [PubMed: 21690353]

Zagotta WN, Hoshi T, Aldrich RW. Shaker potassium channel gating. III: Evaluation of kinetic models for activation. J Gen Physiol. 1994; 103:321–362. [PubMed: 8189208]

Highlights

- Rational design of heat and cold-sensitive ion channels.
- Polarity of the residues undergoing changes in solvation during gating is critical.
- Reduction of gating charge enhances temperature-sensitivity of channel opening.
- Multiple mutations increase temperature-sensitivity in a cumulative manner.

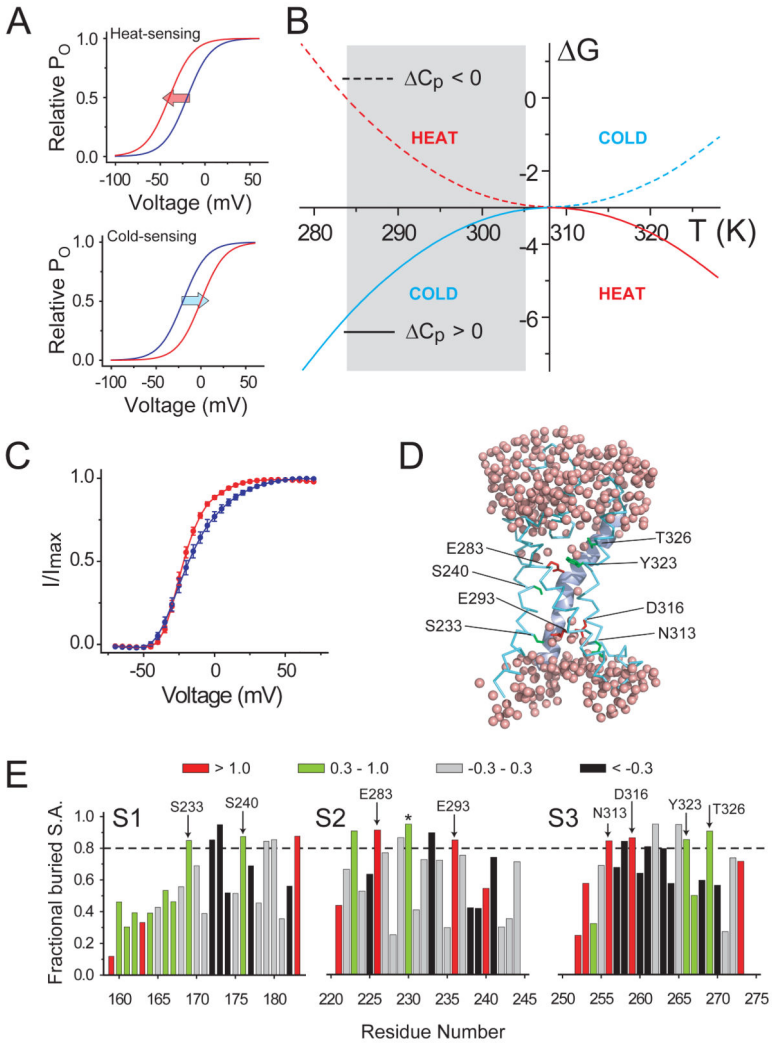

Figure 1. Design template for engineering a temperature modulated ion channel

(A) Arbitrary relative open probability *vs* voltage (P_OV) curves for a heat-sensing channel **(top)** and a cold-sensing channel **(bottom)** at two temperatures (red: high temperature, blue: low temperature). Arrows indicate the shifts in the curve on heating. **(B)** ΔG *vs* T profiles simulated using the equation: $\Delta G(T) = \Delta H_C + \Delta C_P(T-T_C) - T\Delta C_P \ln(T/T_C)$ for two processes, one with a positive ΔC_P (solid curve, ΔC_P = 3 kcal/(mol.K)) and the other with a negative ΔC_P (dotted curve, $\Delta C_P = -3$ kcal/(mol.K)) (see also Fig. S1). In both cases. the critical temperature, T_C, was 308K (35°C), at which the change in enthalpy, ΔH_C, was −3 kcal/mol. The heat sensing and cold sensing regimes of the curves are indicated by the red and blue colors respectively. **(C)** Relative P_OV curve of the wild-type Shaker K_V channel at 28°C (red) and 8°C (blue) (measured from tail currents) (see also Fig. S1). **(D)** A model of a hydrated voltage-sensor, deduced from the crystal structure of the $K_V1.2/2.1$ paddle chimera (see Extended experimental procedures in Supplementary Material), showing occupancy of water within the crevices of the voltage-sensor and the sites that were perturbed in this study. The S4 helix is shown as a cartoon while the S1-S3 helices are shown as ribbons. **(E)** Fractional buried surface area of different residues in the transmembrane segments S1-S3

(residues numbered according the 2R9R structure). The dotted horizontal lines indicate the cut-off for buried surface areas. The bars are colored according to the polarity index of the residue position, deduced from an alignment of 360 K_V channel sequences. Residues targeted in this study are marked with arrows, with the residue numbers corresponding to Shaker K_V channel. The residue marked with an asterisk, while enriched in polar residues in the alignment, is a hydrophobic residue in Shaker K_V channel and was not studied here.

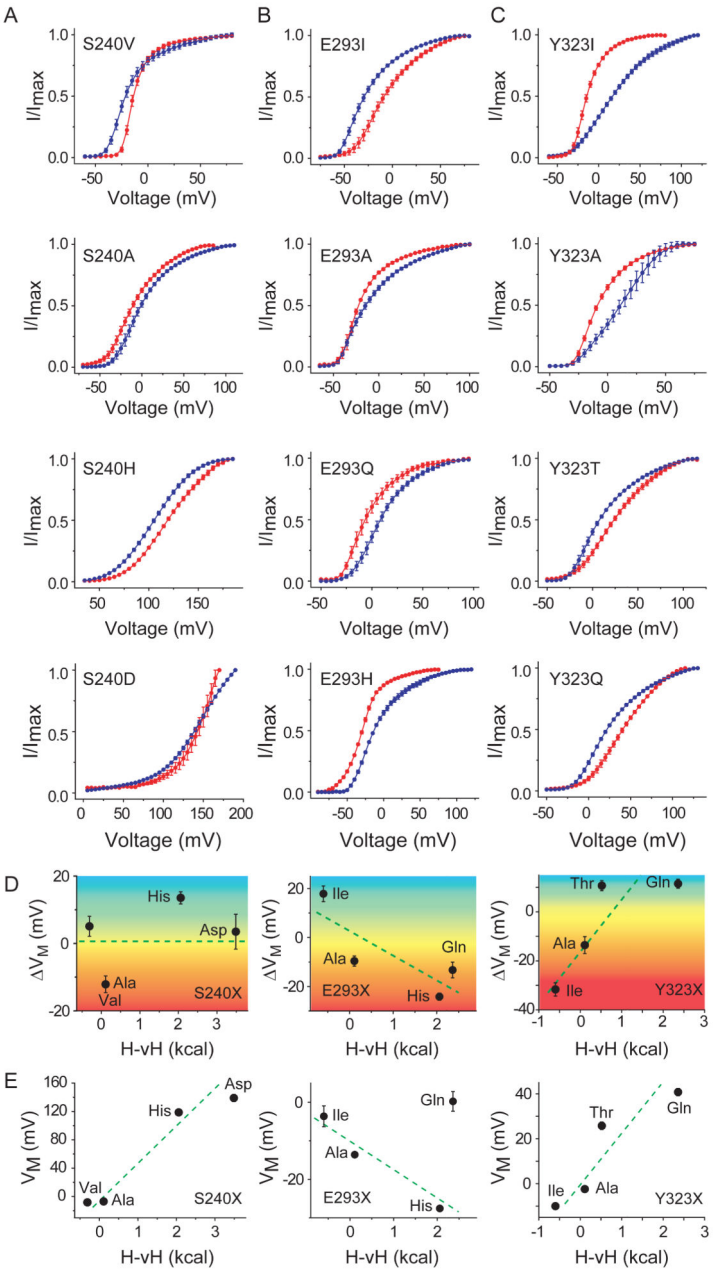

Figure 2. Crevice facing residues of S1-S3 segments sensitize channel opening to temperature

Relative open-probability *vs* voltage-curves for different perturbations at sites S240 **(A)**, E293 **(B)** and Y323 **(C)** mutant, deduced from measurements of tail currents at 5mV voltage intervals (see also Fig. S2). Unless otherwise mentioned, in all cases blue curves indicate measurements at 8°C while red curves indicate measurements at 28°C. The mutation corresponding to each panel is listed in the top left corner of each panel. **(D)** Correlation of temperature dependent change in the median voltage of channel opening (ΔV_M) with the hydrophobicity of perturbation (H-vH scale of biological hydrophobicity (Hessa et al., 2005)) for sites S240 **(left panel)**, E293 **(middle panel)**, Y323 **(right panel)**. The color gradient is used to show the transition from heat (negative ΔV_M) to cold sensitivity (positive

ΔV_M) for the spectrum of mutations. **(E)** Correlation of median voltage of channel opening (V_M) at 28°C, with the hydrophobicity of perturbation for sites S240 **(left panel)**, E293 **(middle panel)**, Y323 **(right panel)**

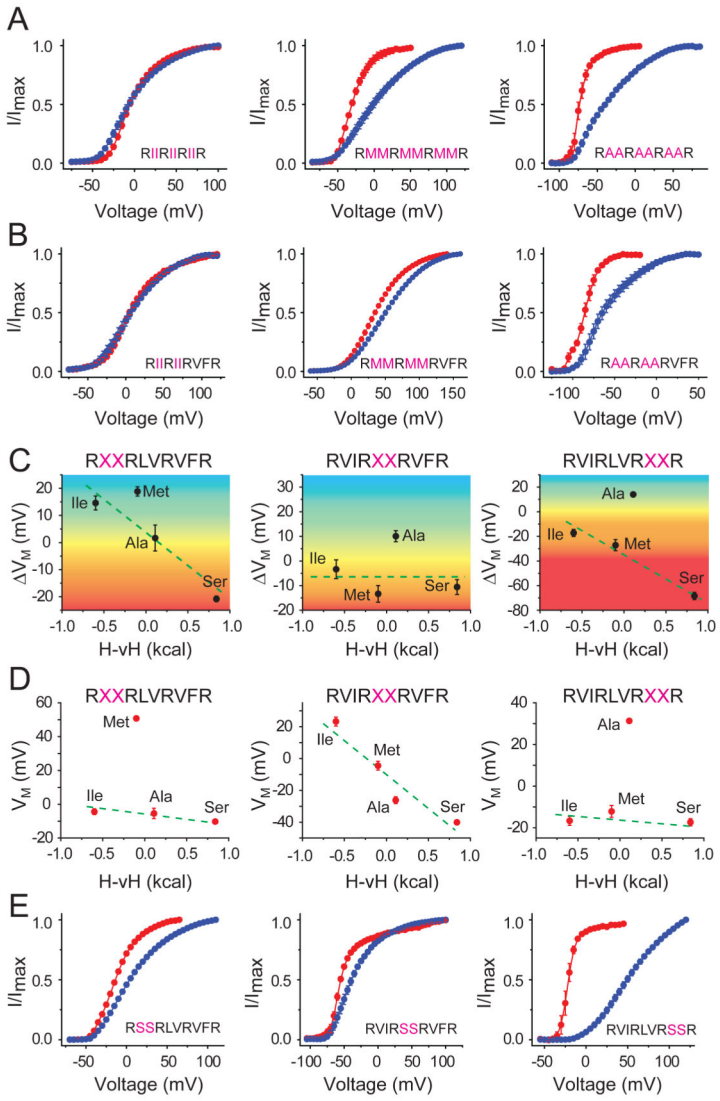

Figure 3. Non-charged residues in S4 segment modulate temperature-sensitivity

(A) Relative P_OV curves, at two temperatures (28°C, red and 8°C, blue) for hextuplet mutations in the S4 segment where six residues are simultaneously mutated to Ile **(left)**, Met **(middle)** or Ala **(right). (B)** Relative P_OV curves, at two temperatures (28°C, red and 8°C, blue) for quadruplet mutations in the S4 segment where four residues are simultaneously mutated to Ile **(left)**, Met **(middle)** or Ala **(right). (C)** Correlation of temperature dependent change in the median voltage of channel opening (ΔV_M) with the hydrophobicity of perturbations for the Top (**left panel**), Middle (**middle panel)** and Bottom (**right panel**) doublet mutations (see also Figs. S3). The color gradient is used to show the transition from heat (negative ΔV_M) to cold sensitivity (positive ΔV_M) for the spectrum of mutations. **(D)** Correlation of median voltage of channel opening (V_M) at 28°C with the hydrophobicity of perturbations for the Top (**left panel**), Middle (**middle panel)** and Bottom (**right panel**) doublet mutations. **(E)** Relative P_OV curves at two temperatures (28°C, red and 8°C, blue) for doublet Ser mutations.

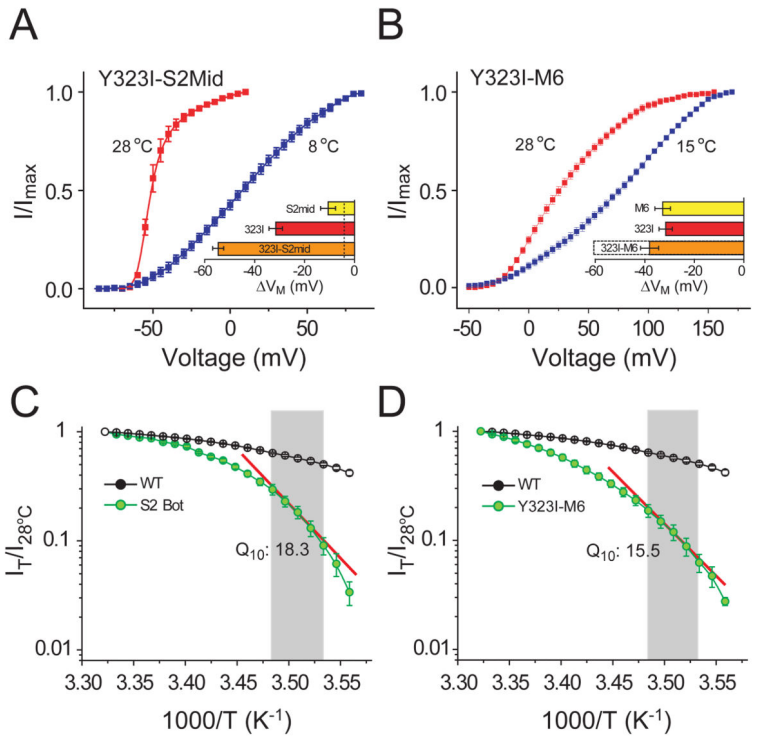

Figure 4. Enhancement of heat sensitivity by combining temperature-sensitive perturbations

(A) Relative P_OV curves for the mutant Y323I-S2Mid at 28°C and 8°C. Horizontal bar plot in the inset shows the temperature dependent shifts (ΔV_M) of the mutant (orange), compared with that of Y323I (red) and S2Mid (yellow). **(B)** Relative P_OV curves for the mutant Y323I-M6 at 28°C and 15°C. Horizontal bar plots in the inset show the shifts in the median voltage of activation (ΔV_M) for Y323I-M6 (orange), Y323I (red) and M6 (yellow). For the Y323I and M6 the shifts correspond to 20°C change in temperature while for the Y323I-M6 the orange bar corresponds to a 13°C change in temperature (the dotted bar corresponds to the shift of the mutant for a 20°C change in temperature expected from a linear extrapolation of the experimental result). **(C) and (D)** Semi-logarithmic plots of fractional outward current, at -20 mV, at different temperatures *vs* inverse of temperature, measured over 28°C to 8°C, at 1°C intervals, for S2Bot **(C)** and Y323I-M6 **(D)** compared with that of the wild-type channel. Shaded region indicates the 10° - 14°C temperature regime over which the Q_{10} value was calculated. Using the formula: $\Delta H = RT^2 \ln Q_{10}/10$ described by Clapham and Miller (2011), the ΔH for the two mutants (at -20mV and room temperature, 20°C) are calculated to be 49.9 kcal/mol (for S2Bot, **(C)**) and 48.5 kcal/mol (for Y323I/M6 **(D)**).

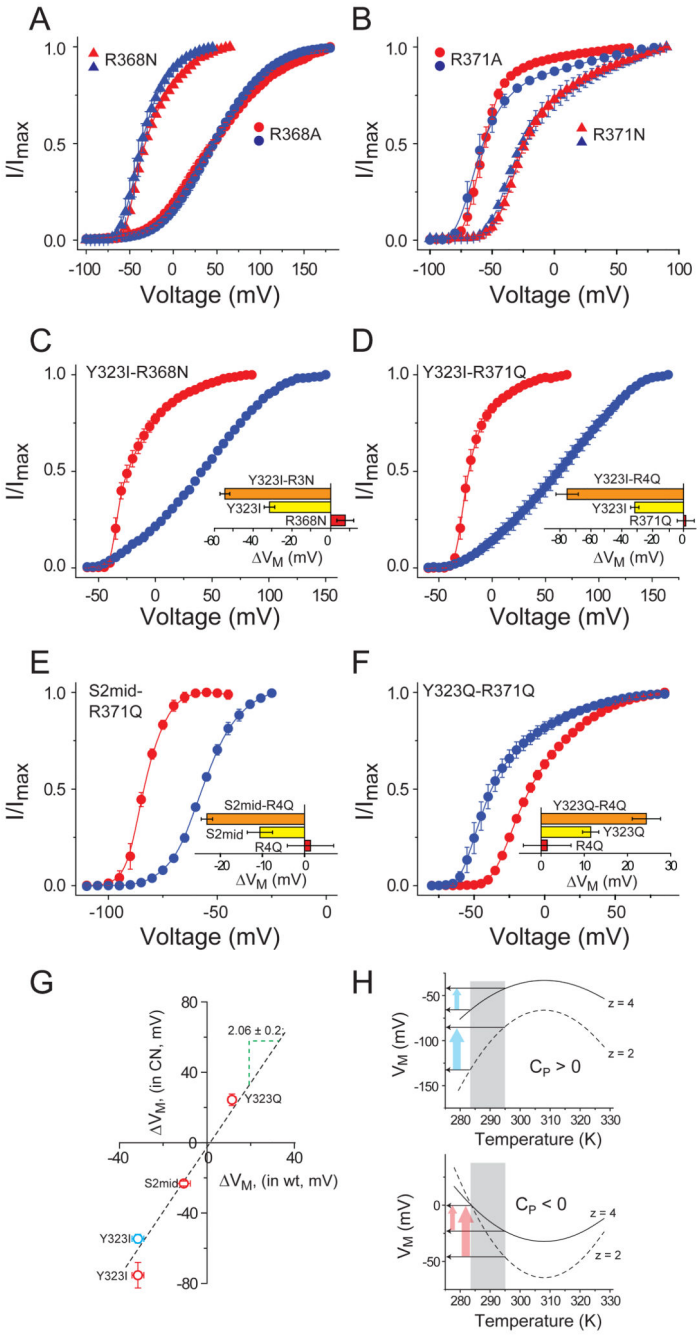

Figure 5. Influence of voltage-sensing charges on temperature sensitivity

(A) Relative P_OV curves of R368N (triangles) and R368A (circles) at 28°C (red) and 8°C (blue) **(B)** Relative P_OV curves of R371Q (triangles) and R371A (circles) at 28°C (red) and 8°C (blue) (see also Fig. S4). **(C)-(F)** Relative P_OV curves of a temperature sensitizing mutant (Y323I, **(C), (D)**; S2mid **(E)**; Y323Q **(F)**) in the background of a charge neutralizing mutant (R368N, **(D)**; R371Q, **(D)-(F)**). In each case the inset shows the temperature induced ΔV_M for the charge neutralizing mutant in red, the temperature sensitizing mutant in yellow and the combination mutant in orange. **(G)** ΔV_M for each of the temperature sensitizing

mutants (Y323I, S2mid, Y323Q) in the background of a gating charge neutralization mutant (R368N (blue circle) or R371Q (red circles)) plotted against ΔV_M for each of the temperature sensitizing mutants (Y323I, S2mid, Y323Q) in the background of the native channel. The dotted line represents the regression line through the points, which has a slope of 2.06 ± 0.2. **(H)** Simulated V_M *vs* temperature profile for a cold sensitive process ($\Delta C_P > 0$, top panel) and a heat sensitive process ($\Delta C_P < 0$, bottom panel), deduced using the equation: $V_M(T) = \{\Delta H_C + \Delta C_P(T-T_C) - T\Delta C_P \ln(T/T_C)\}/z$. In each case, dotted curves indicate the profiles for a process with low voltage-sensitivity and solid curves represent a process with high voltage-sensitivity. Arrows indicate the change in the change in V_M due to change in temperature.

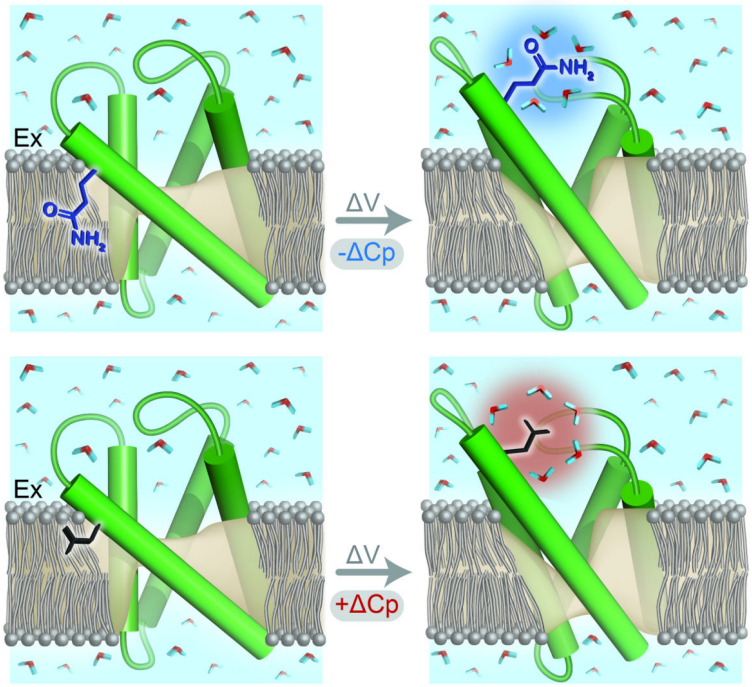

Figure 6. State-dependent change in solvation is a possible mechanism of temperature dependent gating

The cartoons **(Top) and (Bottom)** depict the voltage-sensors in resting and activated conformations. Voltage-dependent change in the VSD is associated with a change in solvation of a residue. When the residue is polar **(Top)**, activation will be conferred a negative ΔC_P (indicated by the blue halo around the hydration shell) and when the residue is non-polar **(Bottom)**, activation will be conferred a positive ΔC_P (indicated by the red halo around the hydration shell). The opposite signs of ΔC_P in the two cases will lead to one of them (**Top)** being heat sensitive and the other **(Bottom)** being cold sensitive.